Observer-Based Assistive Control Design Under Time-Varying Sampling for Power-Assisted Wheelchairs

Guoxi Feng*, Thierry Marie Guerra*, Sami Mohammad, Lucian Busoniu*****

** Univ. Valenciennes, CNRS, UMR 8201 – LAMIH – F59313 Valenciennes, France*
e-mail: {guoxi.feng, guerra}@univ-valenciennes.fr
*** AutoNomad Mobility, Le Mont Houy 59313 Valenciennes Cedex 9, France*
E-mail: sami.mohammad@autonomad-mobility.com
**** Department of Automation, Technical University of Cluj-Napoca, Memorandumului 28, 400114 Cluj-Napoca, Romania*
e-mail: lucian@busoniu.net

Abstract: Compared to manual wheelchairs and fully electric powered wheelchairs, power-assisted wheelchairs (PAWs) provide a special structure where the human can use her/his propulsion to interact with the assistive system. In this context, different studies have focused on the assistive control of PAWs in recent years. This paper presents an observed-based assistive control design using only position encoders. With a time-varying sampling induced by these position encoders, the wheelchair is described by a discrete-time Linear Parameter Varying model. Based on a Takagi-Sugeno (TS) representation, an observer is designed by using LMI techniques. According to the estimated human torques, we use the frequencies with which the wheels are pushed to compute the reference velocity of the centre of gravity. The wheelchair turns with a constant yaw velocity when one of two wheels is braked by the human. Reference tracking is accomplished by a PI controller. Simulation results confirm that the proposed assistive control algorithm provides a good maneuverability for users to control the velocity of the centre of gravity and the yaw velocity of the wheelchair.

Keywords: Assistive control, Disabled persons, State observer, Lyapunov function, T-S model, LMIs.

1. INTRODUCTION

Power-assisted wheelchairs (PAWs), such as the motorization kits Duo and Nomad designed by AutoNomad Mobility (Mohammad, et al., 2015), are driven by both human metabolic power and electrical power from a battery. Thanks to this energy storage structure (Guanetti, et al., 2017), PAWs can provide advantages which cannot be provided by traditional wheelchairs. For example, PAWs have a good compromise between rest and physical exercise for users. Consequently, this kind of wheelchairs prevents disabled people from suffering the common issues caused by a long-term use of manual wheelchair, such as rotator cuff tendonitis, lateral epicondylitis and calcific tendonitis (Levy, et al., 2004). Meanwhile, PAWs can also enable users to maintain a desired physical activity level, which cannot be provided by a fully electric powered wheelchair (Rabhi, et al., 2013)(Fattouh, et al., 2004).

In classical PAWs, different sensors are used to estimate the user's intention or obtain the condition of the road (Seki, et al., 2005)(Seki, et al., 2009). Due to the complexity and the high cost of sensors, this kind of PAWs is neither practical nor affordable for most disabled persons. For these reasons, we use "software sensors" via the observer-based approach (Blandeau, et al., 2018) to reconstruct the human torques using only the angular position encoders.

However, the angular position encoders only provide a new measurement at a fixed angular position interval (Phillips, et al., 1995). In other words, the sampling time is time-varying depending on the angular velocity. This time-varying sampling leads to a discrete-time Linear Parameter-Varying (LPV) model for the wheelchair. We use a Takagi-Sugeno (TS) form to represent the discrete-time LPV model (Takagi and Sugeno 1985)(Precup and Hellendoorn 2011). Moreover, the observer gains are obtained via Linear Matrix Inequality (LMI) techniques (Boyd et al. 1994) (Estrada-Manzo, et al., 2016). Compared to the previous work (Feng, et al., 2017), the present work considers a time-varying observer and delayed nonquadratic Lyapunov function to guarantee the convergence of the observer.

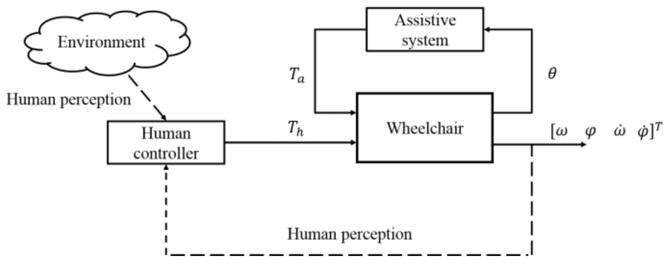

Figure 1: Power-assistance framework

Based on the estimated human torques, the idea is to propose an efficient assistive algorithm in which users can control a PAW depending on their will and perception of the environment. In this framework, shown in Fig 1, users play two important roles. The first role is that of human controller that perceives the environment to generate control signals (human torques). The second role is that of a metabolic energy storage unit. This metabolic energy storage is driven by the state of fatigue which would influence the performance of the human controller. With the help of the assistive algorithm, by observing the states of wheelchair, the state of fatigue and the environment, users can control the velocity and yaw rotation of the wheelchair.

In our proposed approach, the control loop is closed by the user and the assistive torques are generated based on the human torque profiles which are estimated from the angular position signals. Here, it is necessary that the human acting as "the controller" gets information about the surrounding environment to make a decision. Hence, the human can be also considered as an extra "sensor". The advantage of this design is that the human can perceive the information which is difficult or impossible to obtain by conventional sensors. Future trajectory is derived from this information. The assistive system just helps the user to accomplish what he/she is willing to do.

The estimation of the human intention is based on the frequencies and the direction of their torques. For accelerating the wheelchair, users have to push it more frequently, which is detected by a Fast Fourier Transform (FFT). Once running, if no action is detected, the velocity is maintained. Users can brake the right or left wheel to turn right or left respectively. The only way to stop or slow down the wheelchair is to brake both wheels. These four rules govern the assistive system.

The paper is organized as follows. The mechanical dynamics of the power-assisted wheelchair and its corresponding TS representation are introduced in Section 2. Based on the observer, a power-assisted control algorithm is elaborated in Section 3. Simulation results are presented in Section 4 for validating the proposed approaches. Section 5 gives our conclusions.

2. WHEELCHAIR MODELING

2.1 *Mechanical dynamics*

In this study, we consider the wheelchair as a two-wheeled vehicle (Tsai, et al., 2012). The caster's dynamics are not taken into consideration. θ_L and θ_R are respectively the left angular position and the right angular position, r is the wheel radius, d is the distance between two wheels and c is the centre of gravity of the wheelchair with the human.

The two-wheeled PAW can be described by the dynamics:

$$\begin{aligned} \alpha\ddot{\theta}_R + \beta\ddot{\theta}_L &= T_R - K\dot{\theta}_R \\ \alpha\ddot{\theta}_L + \beta\ddot{\theta}_R &= T_L - K\dot{\theta}_L \end{aligned} \tag{1}$$

where the inertial parameters α and β are:

$$\begin{aligned} \alpha &= \frac{mr^2}{4} + \frac{I_C r^2}{b^2} + I_0 \\ \beta &= \frac{mr^2}{4} - \frac{I_C r^2}{b^2} \end{aligned} \tag{2}$$

Here, m, K, I_C, and I_0 denote respectively the mass of wheelchair including the human, the viscous friction coefficient, the inertia of the wheelchair with respect to the vertical axis through c, the inertia of each driving wheel around the wheel axis. T_R and T_L are the total torques exerted on the right wheel and the left wheel respectively. The total torques consists of the unknown torques T_{Rh}, T_{Lh} exerted by user and the assistive torques T_{Rm}, T_{Lm} given by the electrical motors:

$$\begin{aligned} T_R &= T_{Rh} + T_{Rm} \\ T_L &= T_{Lh} + T_{Lm} \end{aligned} \tag{3}$$

The velocity $\dot{\omega}$ of the centre of gravity and the yaw velocity $\dot{\varphi}$ of the wheelchair are the two basic motions which human naturally uses as controlled variables for a desired trajectory. The position of the centre of gravity and the rotation of the wheelchair are respectively ω and φ. These variables can be represented by the angular positions θ_R, θ_L and the angular velocities $\dot{\theta}_R$, $\dot{\theta}_L$ as follows:

$$\begin{bmatrix} \omega \\ \varphi \\ \dot{\omega} \\ \dot{\varphi} \end{bmatrix} = \frac{1}{2} \begin{bmatrix} \begin{matrix} 1 & 1 \\ 1 & -1 \end{matrix} & 0_{2\times 2} \\ 0_{2\times 2} & \begin{matrix} 1 & 1 \\ 1 & -1 \end{matrix} \end{bmatrix} \begin{bmatrix} \theta_R \\ \theta_L \\ \dot{\theta}_R \\ \dot{\theta}_L \end{bmatrix}$$

By choosing the state vector $x^T = [\omega, \varphi, \dot{\omega}, \dot{\varphi}]$, the human torque as inputs $u_h^T = [T_{Rh}, T_{Lh}]$, the motor torque inputs $u_m^T = [T_{Rm}, T_{Lm}]$ and the outputs $y^T = [\theta_R, \theta_L]$, the mechanical system (1) can be rewritten in the following form:

$$\begin{aligned} \dot{x}(t) &= Ax(t) + Bu_h(t) + Bu_m(t) \\ y(t) &= Cx(t) \end{aligned} \tag{4}$$

where the matrices are:

$$A = \begin{bmatrix} 0_{2\times 2} & I_2 \\ 0_{2\times 2} & \begin{matrix} -K/(\alpha+\beta) & 0 \\ 0 & -K/(\alpha-\beta) \end{matrix} \end{bmatrix},$$

$$B = \frac{1}{2}\begin{bmatrix} 0_{2\times 2} \\ 1/(\alpha+\beta) \quad 1/(\alpha+\beta) \\ 1/(\alpha-\beta) \quad 1/(\alpha-\beta) \end{bmatrix} \text{ and } C = \begin{bmatrix} 1 & 1 & 0 & 0 \\ 1 & -1 & 0 & 0 \end{bmatrix}$$

2.2 *Time-varying sampling*

Due to the way the two incremental encoders receive the signals, the sampling period of the angular positions is time varying with the angular velocity. After detecting a rising edge from one of the two angular position sensors, see Fig 2, the system updates the state of the discrete system with the new measurement. The angular velocities are considered as constant between two updates. Therefore, the sampling time s depends on the angular velocities of the two wheels.

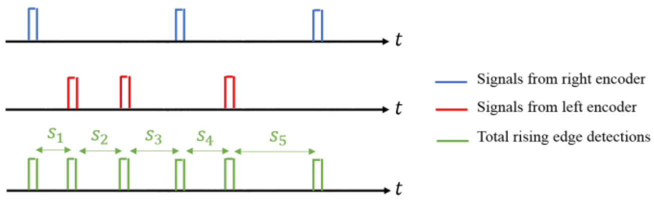

Figure 2: Data sampling example

To derive a discrete-time model, the classical Euler's method is applied with $\dot{x}(t) = (x(k+1) - x(k))/s(\dot{\theta}_R, \dot{\theta}_L)$, where $s(\dot{\theta}_R, \dot{\theta}_L)$ is the sampling time depending on the angular velocities $\dot{\theta}_R$ and $\dot{\theta}_L$. Then, we obtain the discrete-time LPV model as follows:

$$\begin{gathered}\boldsymbol{x}(\boldsymbol{k}+\mathbf{1})=\boldsymbol{A_d}(\boldsymbol{s})\boldsymbol{x}(\boldsymbol{k})+\boldsymbol{B_d}(\boldsymbol{s})[\boldsymbol{u_h}(\boldsymbol{k})+\boldsymbol{u_m}(\boldsymbol{k})]\\ \boldsymbol{y}(\boldsymbol{k})=\boldsymbol{Cx}(\boldsymbol{k})\end{gathered} \tag{5}$$

with the following matrices:

$A_d = s(\dot{\theta}_R, \dot{\theta}_L)A + I_4$, $B_d = s(\dot{\theta}_R, \dot{\theta}_L)B$

Instead of using a predetermined sampling time, this sampling approach updates the state information as soon as a new measurement is received by the system. Compared to the conventional fixed sampling rate, simulation and experimental results (Losero, et al., 2015; Losero, et al., 2016) in the literature show that a satisfying result of the state estimation can be obtained by this approach.

2.3 Polynomial approximation for human torques

We consider that the unknown input torques T_{Rh} and T_{Lh} exerted on the wheels can be approximated by a n_pth degree polynomial function in time, for example for the right wheel $d^{n_p}T_{Rh}/dt^{n_p} = 0$. Using this assumption, the discrete-time input torques dynamic approximation can be expressed as:

$$(\mathbf{1}-\boldsymbol{z}^{-\mathbf{1}})^{\boldsymbol{n_p}}\boldsymbol{T_{Rh}}(\boldsymbol{k})=\mathbf{0} \tag{6}$$

Further, (6) can be expressed as:

$$\boldsymbol{T_{Rh}}(\boldsymbol{k})=-\sum_{\boldsymbol{i=1}}^{\boldsymbol{n_p}}\binom{\boldsymbol{n_p}}{\boldsymbol{i}}(-\mathbf{1})^{\boldsymbol{n_p}}\boldsymbol{T_{Rh}}(\boldsymbol{k}-\boldsymbol{i}) \tag{7}$$

where $\binom{n_p}{i}$ is the binomial coefficient. Consider the unknown input vector $T_{Rh}^{n_p}(k) = [T_{Rh}(k), T_{Rh}(k-1), \ldots, T_{Rh}(k-n_p+1)]^T \epsilon \mathbb{R}^{n_p}$. The dynamics (7) of the vector $T_{Rh}^{n_p}$ can be written as:

$$\boldsymbol{T_{Rh}^{n_p}}(\boldsymbol{k}+\mathbf{1})=\boldsymbol{\Gamma_{n_p}}\boldsymbol{T_{Rh}^{n_p}}(\boldsymbol{k}) \tag{8}$$

where:

$$\Gamma_{n_p}=\begin{bmatrix} -(-1)^1\binom{n_p}{1} & -(-1)^2\binom{n_p}{2} & \cdots & -(-1)^{n_p}\binom{n_p}{n_p} \\ & I_{n_p-1} & & 0_{(n_p-1)\times 1}\end{bmatrix}$$

Applying the same reasoning for the left wheel, the dynamics of the vector $T_{Lh}^{n_p}(k) = [T_{Lh}(k), T_{Lh}(k-1), \ldots, T_{Lh}(k-n_p+1)]^T \epsilon \mathbb{R}^{n_p}$ are:

$$\boldsymbol{T_{Lh}^{n_p}}(\boldsymbol{k}+\mathbf{1})=\boldsymbol{\Gamma_{n_p}}\boldsymbol{T_{Lh}^{n_p}}(\boldsymbol{k}) \tag{9}$$

Defining an extended state vector as $\bar{x} = \left[\omega,\ \varphi, \dot{\omega},\ \dot{\varphi},\ T_{Rh}^{n_p\,T}, T_{Lh}^{n_p\,T}\right]^T \epsilon \mathbb{R}^{2n_p+4}$, the discrete-time LPV system (5) can be rewritten as:

$$\begin{gathered}\bar{\boldsymbol{x}}(\boldsymbol{k}+\mathbf{1})=\bar{\boldsymbol{A}}(\boldsymbol{s})\bar{\boldsymbol{x}}(\boldsymbol{k})+\bar{\boldsymbol{B}}(\boldsymbol{s})\boldsymbol{u_m}(\boldsymbol{k})\\ \boldsymbol{y}(\boldsymbol{k})=\bar{\boldsymbol{C}}\bar{\boldsymbol{x}}(\boldsymbol{k})\end{gathered} \tag{10}$$

where:

$$\bar{A}(s)=\begin{bmatrix} A_d(s) & B_{d1}(s) & 0_{4\times(n_p-1)} & B_{d2}(s) & 0_{4\times(n_p-1)} \\ 0_{n_p\times 4} & & \Gamma_{n_p} & & 0_{n_p\times n_p} \\ 0_{n_p\times 4} & & 0_{n_p\times n_p} & & \Gamma_{n_p}\end{bmatrix},$$

$$\bar{B}(s)=\begin{bmatrix}B_d(s) & 0_{2n_p\times 2}\end{bmatrix}^T, \bar{C}=\begin{bmatrix}C & 0_{2n_p\times 2}\end{bmatrix}.$$

3. ASSISTIVE SYSTEM DESIGN

The assistive system consists in three parts, Fig 2. the human input torques, the velocity and the yaw rotation of the wheelchair are estimated by the observer. According to the frequencies and the direction of the estimated human torques, the algorithm generates the reference signals. Finally, the reference tracking is accomplished by a Proportional-Integral (PI) controller.

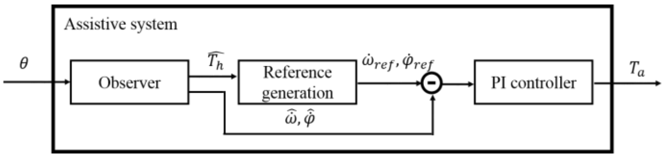

Figure 3: Assistive system overview

3.1 Observer design using TS model

In this section, an unknown input observer for discrete-time LPV system is designed using LMI techniques and last results of Non Quadratic Lyapunov functions (Ding 2010) and delayed Lyapunov functions (Guerra et al. 2012).

Thereinafter, the asterisk $(*)$ represents transposes of a symmetric matrix. For sake of simplicity, we adopt the notations:

$$s = s(k); \quad s^- = s(k-1)$$

The nonlinear term $s(\dot{\theta}_R, \dot{\theta}_L)$ in (10) is the time difference between two consecutive rising edges produced by two encoders. This information can be easily obtained during data acquisition. As the sampling time is bounded (when the angular velocities are not zero), the nonlinear term can be expressed using the classical Sector Nonlinearity Approach (Taniguchi et al. 2001):

$$\boldsymbol{s}(\dot{\boldsymbol{\theta}}_R, \dot{\boldsymbol{\theta}}_L)=\frac{\bar{\boldsymbol{s}}-\boldsymbol{s}(\dot{\boldsymbol{\theta}}_R, \dot{\boldsymbol{\theta}}_L)}{\bar{\boldsymbol{s}}-\underline{\boldsymbol{s}}}\underline{\boldsymbol{s}}+\frac{\boldsymbol{s}(\dot{\boldsymbol{\theta}}_R, \dot{\boldsymbol{\theta}}_L)-\underline{\boldsymbol{s}}}{\bar{\boldsymbol{s}}-\underline{\boldsymbol{s}}}\bar{\boldsymbol{s}} \tag{11}$$

where $\underline{s}$ and $\bar{s}$ are the boundaries of the sampling time i.e. $s(\dot{\theta}_R, \dot{\theta}_L) \in [\underline{s}, \bar{s}]$. Therefore, we can rewrite the nonlinear model (10) as the following TS model:

$$\begin{cases}\bar{x}(k+1)=\bar{A}_s\bar{x}(k)+\bar{B}_s u_m(k)\\ y(k)=\bar{C}\bar{x}(k)\end{cases} \tag{12}$$

With $\bar{A}_s = \sum_{i=1}^{2} h_i\left(s(\dot{\theta}_R, \dot{\theta}_L)\right)A_i$ where $\bar{A}_1 = \bar{A}(\underline{s})$, $\bar{A}_2 = \bar{A}(\bar{s})$, $\bar{B}_1 = \bar{B}(\underline{s})$ and $\bar{B}_2 = \bar{B}(\bar{s})$. The membership functions are:

$$h_1\left(s(\dot{\theta}_R, \dot{\theta}_L)\right)=\frac{\bar{s}-s(\dot{\theta}_R, \dot{\theta}_L)}{\bar{s}-\underline{s}}$$

$$h_2\left(s(\dot{\theta}_R, \dot{\theta}_L)\right)=1-h_1\left(s(\dot{\theta}_R, \dot{\theta}_L)\right)$$

The observer considered for the TS model (12) is:

$$\hat{\bar{x}}(k+1)=\bar{A}_s\hat{\bar{x}}(k)+\bar{B}_s u_m(k)+G_s^{-1}K_{ss^-}\left(y(k)-\hat{y}(k)\right) \tag{13}$$

With for the delayed state the notation:

$$G_{s^-}^{-1}=\left(\sum_{j=1}^{2} h_j(s^-)G_j\right)^{-1};\ K_{ss^-}=\sum_{i}^{2}\sum_{j}^{2} h_i(s)h_j(s^-)K_{ij}$$

G_i and K_{ij}, $i, j = 1, 2$ being free matrices to be derived from the LMI constraints problem. The estimation errors are $e(k) = \bar{x}(k) - \hat{\bar{x}}(k)$. Their dynamics are derived as:

$$\boldsymbol{e}(\boldsymbol{k}+\mathbf{1})=(\bar{\boldsymbol{A}}_{\boldsymbol{s}}-\boldsymbol{G_s^{-1}}\boldsymbol{K_{ss^-}}\bar{\boldsymbol{C}})\boldsymbol{e}(\boldsymbol{k}) \tag{14}$$

The considered delayed nonquadratic Lyapunov function is given by (Guerra et al. 2012):

$$V(e(k),s) = e^T(k)P_{s^-}e(k) \quad (15)$$

In order for the estimation errors to converge to zero, the considered Lyapunov function (16) must decrease along the trajectories of (15). The variation of (16) is negative if the following inequality holds:

$$\begin{bmatrix} -P_{s^-} & (*) \\ G_{s^-}\bar{A}_s - K_{ss^-}\bar{C} & -G_{s^-} - G_{s^-}^T + P_s \end{bmatrix} < 0 \quad (16)$$

We define the following LMI term:

$$\gamma_{ij} = \begin{bmatrix} -P_j & (*) \\ G_j\bar{A}_i - K_{ij}\bar{C} & -G_j - G_j^T + P_i \end{bmatrix} < 0 \quad (17)$$

Theorem 1 (Guerra et al., 2012): The estimation error (15) is globally asymptotically stable if there exist some matrices G_j, P_i and K_{ij} for all $i, j \epsilon \{1,2\}$ such that the LMI conditions γ_{ij} in (18) hold.

The complete proof and more details can be found in (Guerra et al., 2012). Applying Theorem 1, the observer gains (14) can be found by computing the LMIs (18).

3.2 Reference generation

Based on the estimated human torques, a reference generation algorithm is introduced in this section. The proposed power assisted control method is to make the wheelchair more manoeuvrable for the user. More precisely, the velocity, yaw rotation of the wheelchair can be efficiently controlled by human torques. Since the goal is neither to use a torque sensor, nor to have a precise wheelchair + human model, it is impossible to reconstruct a precise amplitude of the human torques. Our reference generation algorithm is based merely on the direction and the frequencies of the human torques estimated from angular positions.

We consider that the frequencies of the human torque range between 0.2-2 Hz which represents approximatively the frequency of propulsion performed by normal users (Boninger, et al., 2000). Consequently, the undesired high frequency components in the estimated signals are filtered automatically. Then, the frequencies are reconstructed by the real-time FFT. The system performs an FFT over a predefined time interval by using the windowing technique. This technique provides a "view" of data through the time interval so called window.

The assistive algorithm should be simple and efficient enough to give users a natural way to control the wheelchair. A higher frequency of users' propulsions leads a higher velocity $\dot{\omega}_{ref}$ of the wheelchair. We design here the reference velocity $\dot{\omega}_{ref}$ is proportional (with a ratio δ) to the highest frequency of left/right hand propulsions. Even if users do not push symmetrically, the assistive algorithm makes the wheelchair go straight. Braking one of the two wheels gives the way to turn. The desired angle to turn depends on how long users brake. If users push less frequently or do not push anymore, the reference velocity keeps constant. To brake or stop the wheelchair (excepted emergency stop provided by a specific device), users should brake both wheels. This action reduces the reference velocity $\dot{\omega}_{ref}$ with a constant rate β. The whole algorithm is shown in Fig. 4.

This new mechanism enables the users to control actively velocity, braking and rotation by changing the frequencies and direction of their propulsions. It is worth noting that the reference generation does not depend on the amplitude of the estimated human torques. Moreover, there are only three parameters α, β and δ to tune. These advantages make the algorithm easy to generalize to different kinds of wheelchairs and users.

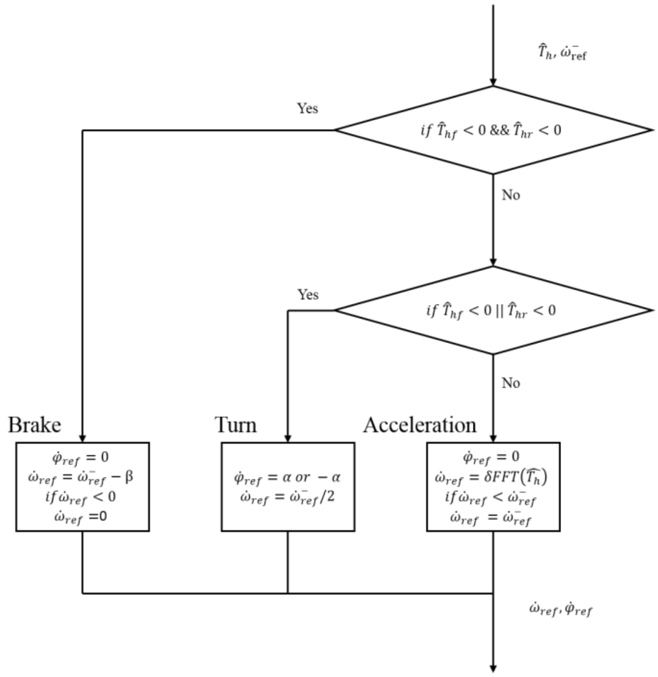

Figure 4: Reference generation diagram

4. SIMULATION

In this section, the proposed observer and power-assisted algorithm are validated by numerical simulations. The goal is to follow the given reference trajectory (or the desired trajectory of the user) under the proposed assistive algorithm and the considered wheelchair dynamics. The human torque control signals are generated directly by a user. The interaction between the user and the virtual simulation is realised by the keyboard and screen as shown figure 5. Here, the PAW is assumed to move on a flat surface. The profile of the human torques are represented by the positive half cycle of a sinusoidal. To perform the trajectory tracking, the user receives the trajectory of the wheelchair from screen and changes the frequencies and the direction of propulsions by keyboard.

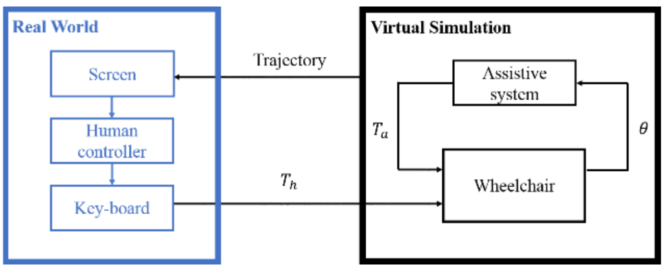

Figure 5: Simulation structure

The following parameters are used to carry out the simulation. $m = 120kg$, $I_C = 40kg.m^2$, $I_0 = 0.25kg.m^2$,

$b = 0.55m$, $r = 0.265m$ and $K = 3N.m.s$. Regarding the observer structure, a second degree polynomial is applied for the approximating function (7). $\underline{s}$ and $\overline{s}$ are respectively *0.001s* and *0.5s*. For the reference generation, we use $\alpha = 0.7854$, $\beta = 0.01$ and $\delta = 2$. Regarding the FFT, we choose a time interval of $10s$ for the window. Before collecting enough data, we initialize the reference velocity as $\dot{\omega}_{ref}(0) = 0.2m/s$ for the 10 first seconds. The PI controller gains are obtained via pole placement including, of course, an anti-wind-up structure.

4.1 Observer validation without power-assistance

Four sequences (green, blue, black and red) of human torque are presented in Fig. 6. They represent respectively the sequence of acceleration, turn right, turn left and brake. As shown in Fig. 6. The observer can qualitatively reconstruct the human torque in terms of frequencies and directions of the propulsions.

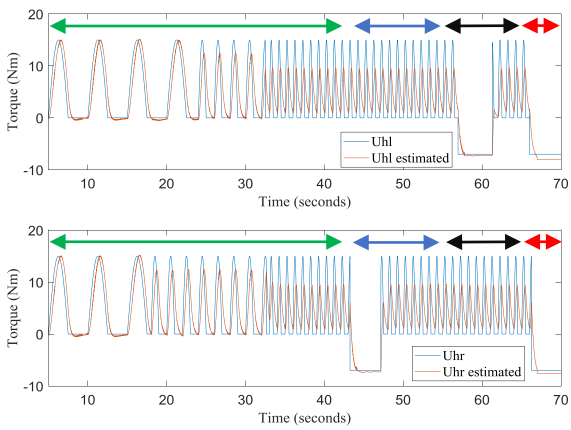

Figure 6: Human torque reconstruction without assistance

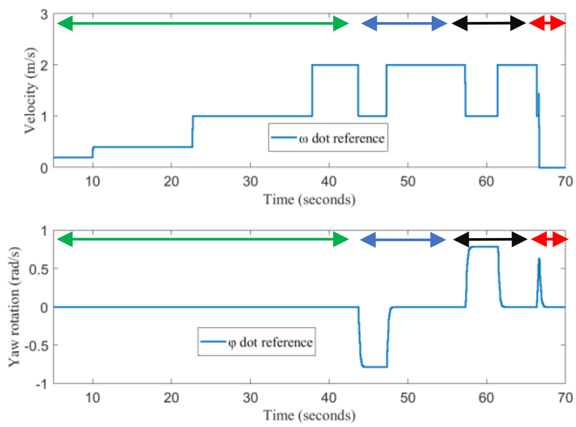

Figure 7: Reference signals generated from the previous estimated human torques

4.2 Reference generation validation without power-assistance

We feed the estimated human torques obtained in the previous part to the reference generation bloc. In the green sequence, the frequencies of the human torque are *0.2Hz*, *0.5Hz* and *1Hz*. As mentioned previously the ratio $\delta = 2$, we notice in Fig. 7 that the reference velocities $\dot{\omega}_{ref}$ are equal to *0.2m/s*, *0.4m/s*, *1m/s* and *2m/s* and correspond to the frequencies of human torque. Also, the reference rotation is $\dot{\varphi}_{ref} = -\alpha$ for $\widehat{U}_{hl} < 0$ and $\dot{\varphi}_{ref} = \alpha$ for $\widehat{U}_{hr} < 0$. In the red sequence, the algorithm detects human wants to stop or brake the wheelchair. Accordingly, $\dot{\omega}_{ref}$ and $\dot{\varphi}_{ref}$ are reduced to 0. Via the proposed observer, the reference generation bloc can provide reference signals for the $\dot{\omega}_{ref}$ and $\dot{\varphi}_{ref}$ desired by the user.

4.3 Predefined trajectory tracking

For this simulation, a predefined trajectory depicted in Fig.8 (including the start point and endpoint) is given. Human should follow this trajectory with the help of the proposed assistive system. The wheelchair has an initial velocity $\dot{\omega}_{ref}(0) = 0.2m/s$.

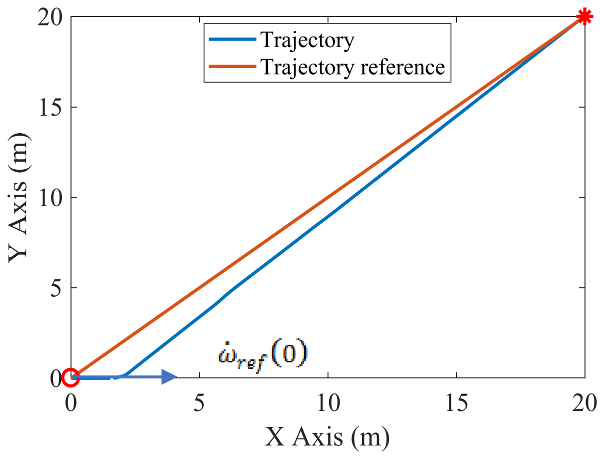

Figure 8: Predefined trajectory tracking performed by a human controller under the proposed assistive algorithm

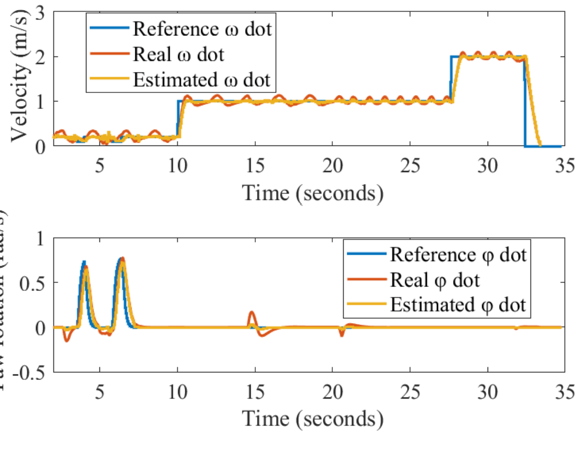

Figure 9: Reference signals and reference tracking performed by a PI controller

As we can see in Fig. 8, the human tries to follow smoothly the trajectory to reach the endpoint. In addition, the human increases gradually the velocity and corrects little by little the direction to point to the endpoint. In Fig. 9, the observer reconstructs successfully the velocity $\dot{\omega}$ and the rotation velocity $\dot{\varphi}$. Moreover, the reference tracking is accomplished by the proposed controller. The small oscillations in $\dot{\omega}$ and

$\dot{\varphi}$ are due to the "strong" human input torques. Another advantage of the assistive system is that the manoeuvrability of the wheelchair does not depend on how strongly the users push. It depends only on the frequency and the direction of propulsion. That is to say, the person who does not have the capacity to provide a strong propulsion (due to fatigue or pathologies) can manipulate the wheelchair as well as a physically strong person. On the other hand, if users are motivated to do physical exercise, they can always provide a desired propulsion to complete the assistive torques.

5. CONCLUSIONS

In this paper, we have presented an observer-based assistive control design for PAWs. To address the time-varying sampling period of the positions encoders, we derive a LPV model for wheelchair. Next, an observer has been proposed to reconstruct the human torques. We use the frequency of the estimated human torques to compute the reference velocity and the reference rotation. Simulation results show the validity of the observer and of the reference generation. Using the assistive system, the human reaches the endpoint trying to follow the given trajectory. This assistive control design not only reduces the system cost by removing the need of torque sensors, but also increases the manoeuvrability of the wheelchair for different kind of users. For future work, a learning algorithm which is able to adapt to each different user can be integrated into the present assistive control algorithm.

ACKNOWLEDGMENT

This research is sponsored by the French Ministry of Higher Education and Research, the National Centre for Scientific Research (CNRS), the Nord-Pas-de-Calais Region. The authors gratefully thank also the AutoNomad company for their expert support in this research work.

REFERENCES

Blandeau, M., Estrada-Manzo, V., Guerra, T. M., Pudlo, P., Gabrielli, F. (2018). Fuzzy unknown input observer for understanding sitting control of persons living with spinal cord injury. *Engineering Applications of Artificial Intelligence*, *67*, 381-389.

Boninger, M. L., Baldwin, M., Cooper, R. A., Koontz, A., Chan, L. (2000). Manual wheelchair pushrim biomechanics and axle position. *Archives of physical medicine and rehabilitation*, *81*(5), 608-613.

Ding B. (2010), Homogeneous polynomially nonquadratic stabilization of discrete-time Takagi-Sugeno systems via nonparallel distributed compensation law, IEEE T. of Fuzzy Systems 18 (5) 994–1000

Estrada-Manzo, V., Lendek, Z., Guerra, T. M. (2016). Generalized LMI observer design for discrete-time nonlinear descriptor models. *Neurocomputing*, *182*, 210-220.

Fattouh, A., Sahnoun, M., & Bourhis, G. (2004, October). Force feedback joystick control of a powered wheelchair: Preliminary study. In *Systems, Man and Cybernetics, 2004 IEEE International Conference on* (Vol. 3, pp. 2640-2645). IEEE.

Feng, G., Guerra, T. M., Busoniu, L., Mohammad, S. (2017). Unknown input observer in descriptor form via LMIs for power-assisted wheelchairs. In *Control Conference (CCC), 36th Chinese* (pp. 6299-6304). IEEE.

Guerra T.M., Kerkeni H., Lauber J., Vermeiren L. (2012). An efficient Lyapunov function for discrete T–S models: observer design. IEEE T. Fuzzy Systems 20 (1), 187-192.

Guanetti, J., Formentin, S., Corno, M., & Savaresi, S. M. (2017). Optimal energy management in series hybrid electric bicycles. *Automatica*, *81*, 96-106.

Levy, C.E., Chow, J.W. (2004). Pushrim-activated power-assist wheelchairs: elegance in motion. *American journal of physical medicine & rehabilitation*, *83*(2), 166-167.

Losero, R., Lauber, J., Guerra, T.M. (2015). Discrete Angular Torque Observer Applicated to the engine torque and clutch torque estimation via a dual-mass flywheel. In *Industrial Electronics and Applications (ICIEA), 2015 IEEE 10th Conference on* (pp. 1020-1025). IEEE.

Losero, R., Lauber, J., Guerra, T. M., Maurel, P. (2016). Dual clutch torque estimation Based on an angular discrete domain Takagi-Sugeno switched observer. In *Fuzzy Systems FUZZ'IEEE* pp. 2357-2363

Mohammad, S., Guerra, T. M., Pudlo, P. (2015), Method and device assisting with the electric propulsion of a rolling system, wheelchair kit comprising such a device and wheelchair equipped with such a device. Patent WO2015173094 A1, issued 19.11.2015

Phillips, A. M., Tomizuka, M. (1995). Multirate estimation and control under time-varying data sampling with applications to information storage devices. In *American Control Conference*, (6), pp. 4151-4155). IEEE.

Precup R-E,, Hellendoorn H., (2011), A survey on industrial applications of fuzzy control. Computers in Industry, 62, pp. 213-226.

Rabhi, Y., Mrabet, M., Fnaiech, F., & Gorce, P. (2013, October). Intelligent joystick for controlling power wheelchair navigation. In *Systems and Control (ICSC), 2013 3rd International Conference on* (pp. 1020-1025). IEEE.

Seki, H., Sugimoto, T., Tadakuma, S. (2005). Novel straight road driving control of power assisted wheelchair based on disturbance estimation and minimum jerk control. In *Industry Applications Conference, 2005. Fourtieth IAS Annual Meeting.* (3), pp. 1711-1717. IEEE.

Seki, H., Ishihara, K., Tadakuma, S. (2009). Novel regenerative braking control of electric power-assisted wheelchair for safety downhill road driving. *IEEE Transactions on Industrial Electronics*, *56*(5), 1393-1400.

Taniguchi, T., Tanaka, K. Wang, H. (2001). Model construction, rule reduction and robust compensation for generalized form of Takagi–Sugeno fuzzy systems. *IEEE Trans. Fuzzy Systems*, vol. 9 (2), 525–537.

Takagi, T. and Sugeno, M., (1985) "Fuzzy identification of systems and its applications to modeling and control," *IEEE Trans. Syst., Man Cybern.*, vol.15 (1), 116–132.

Tsai, M. C., Hsueh, P. W. (2012, July). Synchronized motion control for 2D joystick-based electric wheelchair driven by two wheel motors. In *Advanced Intelligent Mechatronics (AIM), 2012 IEEE/ASME* (pp. 702-707).